Inorg. Chem. **2006**, *45*, 6728–6739

^{13}C NMR Studies of the Electronic Structure of Low-Spin Iron(III) Tetraphenylchlorin Complexes

Akira Ikezaki,[†] Mikio Nakamura,*[,†,‡,§] Sandrine Juillard,[||] and Gérard Simonneaux*[,||]

Department of Chemistry, School of Medicine, Toho University, Ota-ku, Tokyo 143-8540, Japan, Division of Chemistry, Graduate School of Science, Toho University, Funabashi 274-8510, Japan, Research Center for Materials with Integrated Properties, Toho University, Funabashi 274-8510, Japan, and Laboratoire Sciences Chimiques de Rennes, UMR CNRS 6226, Université de Rennes 1, 35042 Rennes Cedex, France

Received March 26, 2006

A series of low-spin six-coordinate (tetraphenylchlorinato)iron(III) complexes $[Fe(TPC)(L)_2]^{\pm}$ (L = 1-MeIm, CN^-, 4-CNPy, and ^{t}BuNC) have been prepared, and their ^{13}C NMR spectra have been examined to reveal the electronic structure. These complexes exist as the mixture of the two isomers with the $(d_{xy})^2(d_{xz}, d_{yz})^3$ and $(d_{xz}, d_{yz})^4(d_{xy})^1$ ground states. Contribution of the $(d_{xz}, d_{yz})^4(d_{xy})^1$ isomer has increased as the axial ligand changes from 1-MeIm, to CN^- (in CD_2Cl_2 solution), CN^- (in CD_3OD solution), and 4-CNPy, and then to ^{t}BuNC as revealed by the *meso* and pyrroline carbon chemical shifts; the *meso* carbon signals at 146 and −19 ppm in $[Fe(TPC)(1\text{-MeIm})_2]^+$ shifted to 763 and 700 ppm in $[Fe(TPC)(^t\text{BuNC})_2]^+$. In the case of the CN^- complex, the population of the $(d_{xz}, d_{yz})^4(d_{xy})^1$ isomer has increased to a great extent when the solvent is changed from CD_2Cl_2 to CD_3OD. The result is ascribed to the stabilization of the d_{xz} and d_{yz} orbitals of iron(III) caused by the hydrogen bonding between methanol and the coordinated cyanide ligand. Comparison of the ^{13}C NMR data of the TPC complexes with those of the TPP, OEP, and OEC complexes has revealed that the populations of the $(d_{xz}, d_{yz})^4(d_{xy})^1$ isomer in TPC complexes are much larger than those in the corresponding TPP, OEC, and OEP complexes carrying the same axial ligands.

Introduction

Nature utilizes iron porphyrins as the prosthetic group for the majority of heme proteins involved in oxygen transport, oxygen and peroxide activation, and electron transfer. Thus there is a considerable amount of data for the physical properties of iron porphyrins to explain their biological properties. In contrast, the electronic structure of iron chlorins still represents a recent active and challenging area,[1] because iron chlorins have been identified as the prosthetic groups of a number of heme proteins only in recent years.[2] A chlorin is an hydroporphyrin with one reduced pyrrole double bond in the macrocyle ring.

The family of green heme proteins is now quite large, containing heme d_1, an iron isobacteriochlorin dione, or heme *d*, an iron chlorin, as prosthetic groups.[2] Thus, cytochrome *bd* oxidase is a bacterial terminal oxidase that contains three cofactors: a low-spin heme (*b558*), a high spin heme (*b595*), and a chlorin *d*.[3−5] Whereas X-ray structures have been published for several heme−copper cytochrome *c* oxidases,[6] no crystal structure is available yet for the cytochrome *bd* family. The molecular mechanism of the enzyme action has been studied in much less detail[7,8] than the heme−copper oxidases. Heme *d* has also been found in catalases, such as hydroperoxidase II, from *Escherichia coli*.[9] In contrast to

* To whom correspondence should be addressed. E-mail: mnakamu@med.toho-u.ac.jp (M.N.).
[†] School of Medicine, Toho University.
[‡] Graduate School of Science, Toho University.
[§] Research Center for Materials with Integrated Properties, Toho University.
[||] UMR CNRS 6226, Université de Rennes 1.

(1) Borisov, V. B.; Liebl, U.; Rappaport, F.; Martin, J.-L.; Zhang, J.; Gennis, R. B.; Konstantinov, A. A.; Vos, M. H. *Biochemistry* **2002**, *41*, 1654−1662.
(2) Timkovich, R. *The Porphyrin Handbook*; Academic Press: San Diego, CA, 2003; Vol. 12, pp 123−156.
(3) Sun, J.; Kahlow, M. A.; Kaysser, T. M.; Osborne, J. P.; Hill, J. J.; Rohlfs, R. J.; Hille, R. Gennis, R. B.; Loehr, T. M. *Biochemistry* **1996**, *35*, 2403−2412.
(4) Sun, J.; Osborne, J. P.; Kahlow, M. A.; Kaysser, T. M.; Gennis, R. B.; Loehr, T. M. *Biochemistry* **1995**, *34*, 12144−12151.
(5) Jünemann, S. *Biochim. Biophys. Acta* **1997**, *1321*, 107−127.
(6) Ostermeier, C.; Harrenga, A.; Ermler, U.; Michel, H. *Proc. Natl. Acad. Sci. U.S.A.* **1997**, *94*, 10547−10553.
(7) Jünemann, S.; Butterworth: P. J.; Wrigglesworth, J. M. *Biochemistry* **1995**, *34*, 14861−14867.
(8) Meunier, B.; Madgwick, S. A.; Reil, E.; Oettmeier, W.; Rich, P. R. *Biochemistry* **1995**, *34*, 1076−1083.

10.1021/ic060508o CCC: $33.50
Published on Web 07/26/2006

cytochrome *bd* oxidase, the crystal structure of catalase HP II from *E. coli* has been determined showing a heme *d* prosthetic group with a *cis*-hydroxychlorin γ-spirolactone[10] and a tyrosine as the proximal ligand.[11] A heme *d* prosthetic group with the same configuration has also been found in the crystal structure of *Penicillium vitale* catalase.[12] Evidence favoring coordination of a tyrosinate proximal ligand to the chlorin iron of *E. coli* Hp II catalase was previously proposed by Dawson et al.[13] Sulfmyoglobin [14,15] and sulfhemoglobin[16] are also green heme proteins.

Since the reference paper reported by Holm and coworkers in 1981,[17] many investigations of the NMR and EPR spectra of low-spin iron(III) complexes of reduced porphyrins have been published very recently,[18] by us[19−22] and others.[15,23−32] The nature of the electronic ground state is not always clear, and more information is needed with these systems. Magnetic circular dichroism spectroscopy has also been shown to be of great utility in the identification of proximal and distal axial ligands in chlorin-containing proteins.[33,34] However, only a limited number of iron chlorin complexes such as high-spin iron(II),[35,36] high-spin iron(III),[30,37] (μ-oxo)bis[(tetraphenylchlorin)iron(III)],[38] and low-spin iron(III) tetraphenylchlorin[18] species have been investigated with X-ray crystallography. We now report ^{13}C NMR analyses of a series of low-spin six-coordinated iron(III) tetraphenylchlorin complexes. The purpose of this study is to extend the coverage of the electronic ground state of iron chlorin models using ^{13}C as NMR probes.

Experimental Section

Synthesis. Free base TPC,[39] Fe(TPC)Cl,[40] Fe(TPC)(CF_3SO_3),[19] [Fe(TPC)(1-MeIm)$_2$]Cl,[20] and [Fe(TPC)(^{t}BuNC)$_2$](CF_3SO_3)[19] were prepared as described previously.

[Fe(TPC)(CN)$_2$]NBu$_4$ was prepared by the addition of 550 μL of CD_2Cl_2 to the mixture consisting of Fe(TPC)Cl (30 μmol) and 2.5 equiv of tetrabutylammonium cyanide. The solution was taken into an NMR sample tube for the ^{1}H NMR measurement. The characterization of all the complexes was done by means of ^{1}H and ^{13}C NMR spectra as given in Results and Discussion.

[Fe(TPC)(4-CNPy)$_2$](CF$_3$SO$_3$). Titration experiment revealed that the addition of 10 equiv of 4-CNPy is enough for the complete conversion of Fe(TPC)(CF_3SO_3) to [Fe(TPC)(4-CNPy)$_2$](CF_3SO_3). Thus, the sample for the NMR measurement was prepared by the addition of 550 μL of CD_2Cl_2 to the mixture consisting of Fe(TPC)(CF_3SO_3) (54 μmol) and 10 equiv of 4-CNPy placed in a reaction vial. The solution was then taken into an NMR sample tube.

***meso*-^{13}C-Enriched [Fe(TPC)(1-MeIm)$_2$]Cl and [Fe(TPC)(CN)$_2$]NBu$_4$.** *meso*-^{13}C-enriched free base TPC was prepared using ^{13}C-enriched benzaldehyde and pyrrole according to the literature.[39] It was then converted to Fe(TPC)Cl by the literature method.[40] *meso*-^{13}C-enriched [Fe(TPC)(1-MeIm)$_2$]Cl was prepared by the addition of 550 μL of CD_2Cl_2 to the mixture consisting of *meso*-^{13}C-enriched Fe(TPC)Cl (14 μmol) and 4 equiv of 1-MeIm placed in a reaction vial. *meso*-^{13}C-enriched [Fe(TPC)(CN)$_2$]NBu$_4$ was similarly prepared from 4 equiv of tetrabutylammonium cyanide and *meso*-^{13}C-enriched Fe(TPC)Cl(14 μmol).

***meso*-^{13}C-Enriched Fe(TPC)ClO$_4$.** To the mixture of $AgClO_4$ (69 μmol) and Fe(TPC)Cl (57 μmol) was added 10 mL of THF. The solution was stirred for 20 min at room temperature. After evaporation of the solvent, dichloromethane (3 mL) was added to the resultant solid and the suspension was filtered to remove AgCl. This procedure was repeated twice. The filtrate was evaporated, and the resultant solid was dried in vacuo for 4 h at 25 °C. The prechlorate salt, Fe(TPC)ClO_4, thus obtained was used without further purification.

Caution! Perchlorate salts are potentially explosive when heated or shocked. Handle them in milligram quantities with care.

(9) Chiu, J. T.; Loewen, P. C.; Switala, J.; Gennis., R. B.; Timkovich, R. *J. Am. Chem. Soc.* **1989**, *111*, 7046−7050.
(10) Andersson, L. A.; Sotiriou, C.; Chang, C. K.; Loehr, T. M. *J. Am. Chem. Soc.* **1987**, *109*, 258−264.
(11) Bravo, J.; Verdaguer, N.; Tormo, J.; Betzel, C.; Switala, J.; Loewen, P. C.; Fita, I. *Structure* **1995**, *3*, 491−502.
(12) Murshudov, G. N.; Grebenko, A. I.; Barynin, V.; Dauter, Z.; Wilson, K. S.; Vainshtein, B. K.; Melik-Adamyan, W.; Bravo, J.; Ferrán, J. M.; Ferrer, J. C.; Switala, J.; Loewen, P. C.; Fita, I. *J. Biol. Chem.* **1996**, *271*, 8863−8868.
(13) Dawson, J. H.; Bracete, A. M.; Huff, A. M.; Kadkhodayan, S.; Zeitler, C. M.; Sono, M.; Chang, C. K.; Loewen, P. C. *FEBS Lett.* **1991**, *295*, 123−126.
(14) Bondoc, L. L.; Chau, M. H.; Price, M. A.; Timkovich, R. *Biochemistry* **1986**, *25*, 8458−8466.
(15) Chatfield, M. J.; La Mar, G. N.; Parker, W. O.; Smith, K. M.; Leung, H.-K.; Morris, I. K. *J. Am. Chem. Soc.* **1988**, *110*, 6352−6358.
(16) Chatfield, M. J.; La Mar, G. N. *Arch. Biochem. Biophys.* **1992**, *295*, 289−296.
(17) Stolzenberg, A. M.; Strauss, S. H.; Holm, R. H. *J. Am. Chem. Soc.* **1981**, *103*, 4763−4778.
(18) Kobeissi, M.; Toupet, L.; Simonneaux, G. *Inorg. Chem.* **2001**, *40*, 4494−4499.
(19) Simonneaux, G.; Kobeissi, M. *J. Chem. Soc., Dalton Trans.* **2001**, 1587−1592.
(20) Simonneaux, G.; Kobeissi, M.; Toupet, L. *J. Chem. Soc, Dalton Trans.* **2002**, 4011−4016.
(21) Kobeissi, M.; Simonneaux, G. *Inorg. Chim. Acta* **2003**, *343*, 18−26.
(22) Simonneaux, G.; Kobeissi, M.; Toupet, L. *Inorg. Chem.* **2003**, *42*, 1644−1651.
(23) Muhoberac, B. B. *Arch. Biochem. Biophys.* **1984**, *233*, 682−697.
(24) Morishima, I.; Fujii, H.; Shiro, Y. *J. Am. Chem. Soc.* **1986**, *108*, 3858−3860.
(25) Licoccia, S.; Chatfield, M. J.; La Mar, G. N.; Smith, K. M.; Mansfield, K. E.; Anderson, R. R. *J. Am. Chem. Soc.* **1989**, *111*, 6087−6093.
(26) Keating, K. A.; de Ropp, J. S.; La Mar, G. N.; Balch, A. L.; Shiau, F. Y.; Smith, K. M. *Inorg. Chem.* **1991**, *30*, 3258−3263.
(27) Ozawa, S.; Watanabe, Y.; Morishima, I. *Inorg. Chem.* **1992**, *31*, 4042−4043.
(28) Ozawa, S.; Watanabe, Y.; Morishima, I. *J. Am. Chem. Soc.* **1994**, *116*, 5832−5838.
(29) Jayaraj, K.; Gold, A.; Austin, R. N.; Mandon, D.; Weiss, R.; Terner, J.; Bill, E.; Müther, M.; Trautwein, A. X. *J. Am. Chem. Soc.* **1995**, *117*, 9079−9080.
(30) Wojaczyński, J.; Latos-Grażyński, L.; Głowiak, T. *Inorg. Chem.* **1997**, *36*, 6299−6306.
(31) Astashkin, A. V.; Raitsimring, A. M.; Walker, F. A. *J. Am. Chem. Soc.* **2001**, *123*, 1905−1913.
(32) Cai, S.; Lichtenberger, L.; Walker, F. A. *Inorg. Chem.* **2005**, *44*, 1890−1903.
(33) Huff, A. M.; Chang, C. K.; Cooper, D. K.; Smith, K. M.; Dawson, J. H. *Inorg. Chem.* **1993**, *32*, 1460−1466.
(34) Bracete, A. M.; Kadkhodayan, S.; Sono, M.; Huff, A. M.; Zhuang, C.; Cooper, D. K.; Smith, K. M.; Chang, C. K.; Dawson, J. H. *Inorg. Chem.* **1994**, *33*, 5042−5049.
(35) Strauss, S. H.; Silver, M. E.; Ibers, J. A. *J. Am. Chem. Soc.* **1983**, *105*, 4108−4109.
(36) Strauss, S. H.; Silver, M. E.; Long, K. M.; Thompson, R. G.; Hudgens, R. A.; Spartalian, K.; Ibers, J. A. *J. Am. Chem. Soc.* **1985**, *107*, 4207−4215.
(37) Jayaraj, K.; Gold, A.; Austin, R. N.; Ball, L. M.; Terner, J.; Mandon, D.; Weiss, R.; Fischer, J.; DeCian, A.; Bill, E.; Müther, M.; Schünemann, V.; Trautwein, A. X. *Inorg. Chem.* **1997**, *36*, 4555−4566.
(38) Strauss, S. H.; Pawlik, M. J.; Skowyra, J.; Kennedy, J. R.; Anderson, O. P.; Spartalian, K.; Dye, J. L. *Inorg. Chem.* **1987**, *26*, 724−730.
(39) Whitlock, H. W., Jr.; Hanauer, R.; Oester, M. Y.; Bower, B. K. *J. Am. Chem. Soc.* **1969**, *91*, 7485−7489.
(40) Feng, D.; Ting, Y.-S.; Ryan, M. D. *Inorg. Chem.*, **1985**, *24*, 612−617.

***meso*-^{13}C-Enriched [Fe(TPC)(4-CNPy)$_2$]ClO$_4$ and [Fe(TPC)-(^{t}BuNC)$_2$]ClO$_4$.** *meso*-^{13}C-enriched [Fe(TPC)(4-CNPy)$_2$]ClO$_4$ was prepared by the addition of 550 μL of CD_2Cl_2 to the mixture consisting of Fe(TPC)ClO$_4$(13 μmol) and 10 equiv of 4-CNPy. The solution was taken into an NMR sample tube for the NMR measurement. *meso*-^{13}C-enriched [Fe(TPC)(^{t}BuNC)$_2$]ClO$_4$ was similarly prepared from 3 equiv of ^{t}BuNC and Fe(TPC)ClO$_4$ (26 μmol).

[Co(TPC)(CN)$_2$]NBu$_4$. Free base chlorin was treated with 13 equiv of $CoCl_2 \cdot 6H_2O$ in refluxing $CHCl_3-CH_3OH$ (3:1) solution for 4 h.[41] The reaction mixture was washed with water to remove the inorganic material. The organic layer was dried over sodium sulfate for 1 h. The solution was evaporated to dryness, and the resultant cobalt(II) complex, Co(TPC), was dried in vacuo for 4 h at 25 °C. The solid still contained some amount of free base. Thus, the reaction was repeated for the complete conversion of the free base to the cabalt(II) complex. To a 550 μL volume of CD_2Cl_2 solution of Co(TPC) (15 μmol) was added a CD_2Cl_2 solution containing 2.5 equiv of tetrabutylammonium cyanide. The solution, after being stirred for 1 h in a vial, gave cobalt(III) complex [Co(TPC)(CN)$_2$]NBu$_4$ in a quantitative yield. ^{1}H NMR and ^{13}C NMR chemical shifts determined in CD_2Cl_2 at 298 K are given in Results and Discussion.

NMR Spectroscopy. Samples for NMR studies were prepared by the addition of 550 μL of CD_2Cl_2 to the reaction vial containing Fe(TPC)X and excess ligand under argon atmosphere. ^{1}H and ^{13}C NMR spectra were recorded on a JEOL LA300 spectrometer operating at 300.4 MHz for ^{1}H. Chemical shifts were referenced to the residual peak of dichloromethane-d_2 ($\delta = 5.32$ ppm for ^{1}H and 53.8 ppm for ^{13}C) and methanol-d_4 ($\delta = 3.30$ ppm for ^{1}H and 49.0 ppm for ^{13}C). UV−vis spectra were recorded on a Shimadzu MultiSpec-1500 at ambient temperature.

Results

Assignments of ^{1}H NMR Signals. The ^{1}H NMR spectra of [Fe(TPC)L$_2$]$^+$ where the axial ligands are PMe$_2$Ph,[18] 1-MeIm,[20] P(OMe)$_2$Ph,[21] and ^{t}BuNC[19] have already been reported in detail. In the following discussion, we will describe the signal assignments of three new complexes including diamagnetic [Co(TPC)(CN)$_2$]NBu$_4$.

[Fe(TPC)(CN)$_2$](NBu$_4$). Figure 1 shows the ^{1}H NMR spectra of [Fe(TPC)(CN)$_2$]$^-$ taken in (a) CD_2Cl_2 and (b) CD_3OD solutions at 298 K. Because of the presence of the pyrroline ring, these complexes belong to the C_{2v} point group. Thus, the pyrrole protons give three signals signified as 7,18-H, 8,17-H, and 12,13-H as shown in Chart 1, and the *ortho*, *meta*, and *para* protons give two signals. These signals were assigned on the basis of the relative intensity and multiplicity of each signal together with the 2D COSY experiments. In the case of [Fe(TPC)(CN)$_2$]$^-$ taken in CD_2Cl_2 solution, the pyrrole signal at −1.9 ppm was assigned to the 12,13-H since no cross-peak was observed. In contrast, a cross-peak was observed between the signals at 3.3 and −26.0 ppm (Supporting Information S-1). Thus, these two signals were assigned to the pyrrole protons in the same pyrrole ring; i.e., 7,8-H and 17,18-H. Two sets of the phenyl signals were assigned on the basis of the homonuclear selective decoupling; they are (*o*, *m*, *p*) = (6.38, 7.94, 6.95 ppm) and (6.66, 7.88, 6.88 ppm) (S-2). The complete signal assignment was achieved by the NOE difference spectra. Irradiation of the signal at −1.9 ppm (12,13-H) caused the enhancement of the signal at 6.66 ppm. Thus the signal at 6.66 ppm was assigned to the *ortho*-H of the 10,15-phenyl rings (S-2). Similarly, irradiation of the signal at −26.0 ppm caused the enhancement of the signal at 6.66 ppm (S-2). Thus, the signals at −26.0 and 3.3 ppm were assigned to the 8,17-H and 7,18-H, respectively.

As is clear from Figure 1, the chemical shifts of [Fe(TPC)(CN)$_2$]$^-$ in CD_3OD solution are quite different from those in CD_2Cl_2 solution. The signals observed in CD_3OD solution were similarly assigned on the basis of the relative intensity and multiplicity of each signal, selective homonuclear decoupling, NOE difference spectra (S-3), and 2D

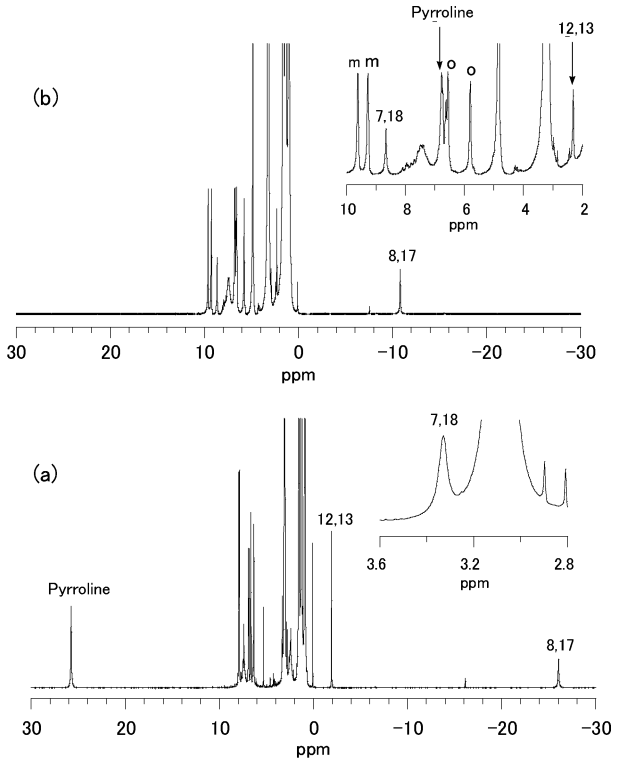

Figure 1. ^{1}H NMR spectra of [Fe(TPC)(CN)$_2$](NBu$_4$) taken in (a) CD_2Cl_2 and in (b) CD_3OD solutions at 298 K. Strong signals ascribed to the butyl protons are observed between 1 and 4.5 ppm.

Chart 1. (a) Atom Numbering and (b) Atom Labeling in [Fe(TPC)L$_2$]$^{\pm}$ with C_{2v} Point Group[a]

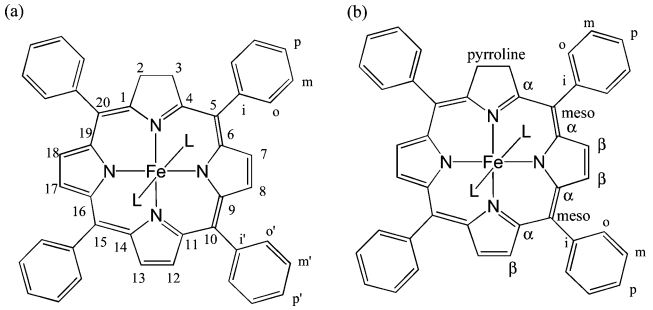

[a] α-C: carbon atoms at the 1, 4, 6, 9, 11, 14, 16, and 19 positions. β-C and β-H: carbon and hydrogen atoms at the 7, 8, 12, 13, 17, and 18 positions, respectively. Pyrroline-C and pyrroline-H: carbon and hydrogen atoms at the 2 and 3 positions, respectively. *meso*: carbon atoms at the 5, 10, 15, and 20 positions.

(41) Karweik, D. H.; Winograd, N. *Inorg. Chem.* **1976**, *15*, 2336−2342.

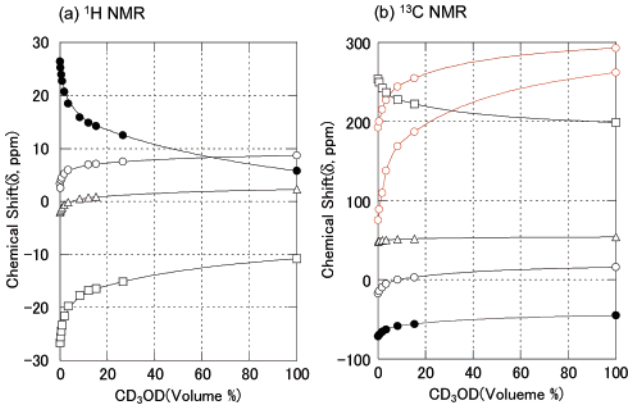

Figure 2. Change in (a) ^{1}H NMR and (b) ^{13}C NMR chemical shifts when CD_3OD is added to the CD_2Cl_2 solution of $[Fe(TPC)(CN)_2]^-$ at 298 K. Symbols in (a): ●, pyrroline-H; ○, 7,18-H; △, 12,13-H; □, 8,17-H. Symbols in (b): ●, pyrroline-C; ○, 7,18-C; △, 12,13-C; □, 8,17-C; red ○, meso-C.

COSY spectra (S-4, S-5). For example, the signal at 8.7 ppm showed a correlation peak with that at −10.8 ppm (S-5). Thus, these signals were assigned to the 7,8,17,18-H. The complete signal assignment was achieved by the NOE difference spectra. Thus, the signals at 8.7 and −10.8 ppm were assigned to the 7,18-H and 8,17-H, respectively. Figure 2a shows the change in chemical shift of the pyrrole and pyrroline-H signals when CD_3OD is added to the CD_2Cl_2 solution of $[Fe(TPC)(CN)_2]^-$ at 298 K. When the volume % of the added CD_3OD reached 15.4%, the pyrrole signals at 3.3, −1.9, and −26.0 ppm shifted to 7.1, 0.9, and −16.4 ppm, respectively. Thus, the signals at 8.7, 2.3, and −10.8 ppm observed in CD_3OD solution correspond to the signals at 3.3, −1.9, and −26.0 ppm observed in CD_2Cl_2 solution, which in turn indicate that they are assigned to 7,18-H, 12,13-H, and 8,17-H, respectively. It should be noted that the spread among the pyrrole signals decreased from 29.3 to 19.5 ppm as CD_2Cl_2 is replaced by CD_3OD. Figure 3a,b shows the Curie plots of the pyrroline and pyrrole-H signals of $[Fe(TPC)(CN)_2]^-$ taken in CD_2Cl_2 and CD_3OD solutions, respectively. In both cases, the chemical shifts vary linearly with $1/T$, but the extrapolated lines do not pass through the diamagnetic value at $1/T = 0$. Especially, the pyrroline and 8,17-H signals showed a large positive and negative slope in CD_2Cl_2 solution, $+2.7 \times 10^4$ and -2.5×10^4 ppm·K, respectively. The intercepts at $1/T = 0$ for these signals reached as much as −67 and 59 ppm, respectively; the chemical shifts of the corresponding signals in diamagnetic $[Co(TPC)(CN)_2]^-$ are 4.0 and 8.4 ppm. In CD_3OD solution, the signs of the Curie slopes of the pyrroline and 8,17-H signals were reversed and their absolute values were diminished to a great extent; they were -1.1×10^4 and $+0.37 \times 10^4$ ppm·K, respectively. The intercepts at $1/T = 0$ for the pyrroline and 8,17-H decreased to 42.4 and −23.5 ppm, respectively. Thus, it is clear that the electronic ground state in CD_2Cl_2 solution is quite different from that in CD_3OD, which will be discussed later.

$[Fe(TPC)(4\text{-}CNPy)_2](ClO_4)$. At ambient temperature, the ligand dissociation in $[Fe(TPC)(4\text{-}CNPy)_2]^+$ is taking place on the ^{1}H NMR time scale to give broad signals ascribed to the free and coordinated ligand molecules. Figure 4 shows the ^{1}H NMR spectrum of $[Fe(TPC)(4\text{-}CNPy)_2]^+$ taken at 253 K where the ligand exchange is slow enough to give clearly resolved signals. These signals were assigned similarly by COSY spectra as in the case of $[Fe(TPC)(CN)_2]^-$ (S-6, S-7). The Curie plots of the pyrroline and pyrrole-H signals are given in Figure 3c. The slopes of the Curie lines are -1.3×10^4 and $+0.41 \times 10^4$ ppm·K, respectively, which are quite close to the corresponding values of $[Fe(TPC)(CN)_2]^-$ in CD_3OD. Thus, the electronic ground state of $[Fe(TPC)(4\text{-}CNPy)_2]^+$ is considered to be similar to that of $[Fe(TPC)(CN)_2]^-$ in CD_3OD.

$[Co(TPC)(CN)_2]NBu_4$. Determination of the ^{1}H NMR chemical shifts of diamagnetic $[Co(TPC)(CN)_2]NBu_4$ is necessary to know the isotropic shifts of paramagnetic $[Fe(TPC)L_2]^{\pm}$. The signal assignment was carried out by means of 1D homonuclear decoupling and NOE difference spectroscopy (S-8) as well as 2D COSY spectroscopy (S-9). The chemical shifts of the *ortho* and *meta* protons in one phenyl ring were determined to be 7.81 and 7.56 ppm, respectively, while those of the other phenyl ring were determined to be 8.00 and 7.63 ppm, respectively, by the COSY spectra (S-9). The *para* signals were almost overlapping with the *meta* signals in each case; they appeared at 7.58 and 7.61 ppm. The NOE difference spectrum showed the increase in intensity of the *ortho* signals at 7.81 ppm when the pyrroline signal at 4.00 ppm was irradiated (S-8). Thus, the signals at 7.81 and 8.00 ppm were ascribed to the *ortho* protons of the 5,20- and 10,15-phenyl groups, respectively. The signals at downfield regions, 8.08 (d) and 8.36 (d) ppm, were assigned to the pyrrole 7,8,17,18-H, while the singlet at 8.28 ppm was assigned to the 12,13-H. The NOE difference spectrum showed the increase in intensity of the pyrrole signals at 8.08 ppm when the *ortho* signals at 7.81 ppm was irradiated. Similarly, the intensity of the pyrrole signals at 8.28 and 8.36 ppm increased when the *ortho* signal at 8.00 was irradiated. Thus, the doublets at 8.08 and 8.36 ppm were assigned to the 7,18-H and 8,17-H, respectively.

The chemical shifts of these complexes are given in Table 1. The axial ligands are arranged in the descending order of the pyrroline shifts, which corresponds to the ascending order of the 8,17-H shifts.

Assignments of ^{13}C NMR Signals. Full analysis of the ^{13}C NMR spectra of low-spin $[Fe(TPC)L_2]^+$ have not been reported before. In the following discussion, we will describe the signal assignments of the complexes carrying 1-MeIm, CN^- in CD_2Cl_2 solution, CN^- in CD_3OD solution, 4-CNPy, and ^{t}BuNC as axial ligands.

$[Fe(TPC)(CN)_2](NBu_4)$. Figure 5a shows the proton-decoupled ^{13}C NMR spectrum of $[Fe(TPC)(CN)_2]^-$ taken in CD_2Cl_2 solution at 298 K. The α- and *β*-C give four and three signals, respectively, and the *meso*, *ipso*, *o*-, *m*-, and *p*-C give two signals as revealed from Chart 1. Signal assignment of the carbons with directly bonded protons such as pyrroline-*β*, pyrrole-*β*, *o*, *m*, and *p* has been done on the basis of the relative intensity and multiplicity of the signal in the proton coupled spectra together with the ^{1}H{^{13}C} HMQC experiments. For example, the ^{13}C signal at 48 ppm

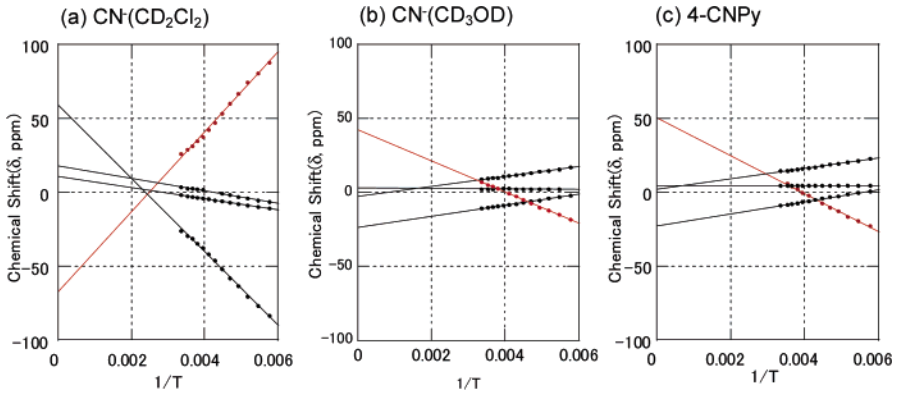

Figure 3. Curie plots of the ^{1}H NMR signals: (a) $[Fe(TPC)(CN)_2]^-$ taken in CD_2Cl_2; (b) $[Fe(TPC)(CN)_2]^-$ taken in CD_3OD; (c) $[Fe(TPC)(4\text{-}CNPy)_2]^+$ taken in CD_2Cl_2. Key: ●, pyrrol-H; red ●, pyrroline-H.

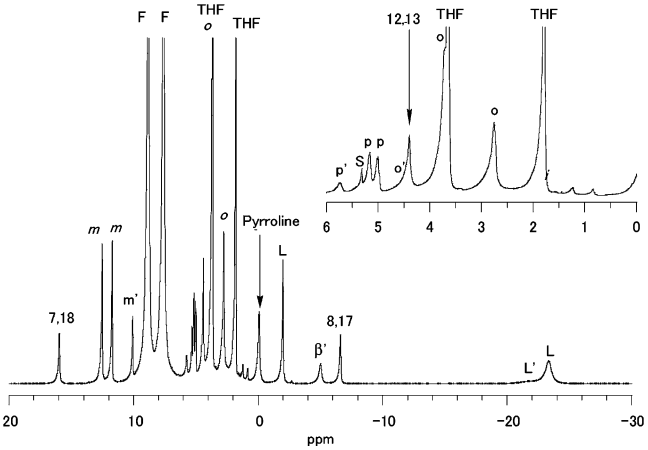

Figure 4. ^{1}H NMR spectrum of $[Fe(TPC)(4\text{-}CNPy)_2]^+$ taken in CD_2Cl_2 at 253 K. Signals signified by L′, *β*′, *o*′, *m*′, and *p*′ in the spectra indicate the ligand, pyrrole-H, and *meta* signals of $[Fe(TPP)(4\text{-}CNPy)_2]^+$. S and F are the signals for the solvent and free ligand, respectively.

in CD_2Cl_2 solution, which showed a correlation peak with the proton signal at −1.9 ppm, was assigned to the 12,13-C (S-10). Similarly, the signals at −17 and 254 ppm were assigned to the 7,18-C and 8,17-C, respectively, since these signals have correlation peaks with the proton signals at 3.3 and −26.0 ppm, respectively (S-11, S-12). The pyrrole-*β* signals were also assigned by the heteronuclear selective decoupling (S-13). The assignments of the α, *meso*, and *ipso* signals are much more difficult. In the inset of Figure 5a′ is given the partially relaxed proton decoupled ^{13}C NMR spectrum, which is obtained by the 180°−*τ*−90° pulse sequence with $\tau = 75$ ms. Because of the short relaxation times of the α, *β*, and *meso* carbons relative to those of the *o*, *m*, *p*, and *ipso* carbons, the former gave positive signals while the latter gave negative ones. Thus, the six unassigned signals in a wide frequency range, i.e., 192, 162, 130, 76, −20, −87 ppm, were assigned either to the *meso* or to the α carbons. As shown in Figure 5a″, we could unambiguously assign the signals at 192 and 76 ppm to the *meso* carbons by using *meso*-^{13}C enriched $[Fe(TPC)(CN)_2]^-$. The other four signals at 162, 130, −20, and −87 ppm were then assigned to the α carbons.

The ^{13}C NMR spectra of $[Fe(TPC)(CN)_2]^-$ taken in CD_3OD solution at 298 K is given in Figure 5b. The *o*, *m*, *p*, pyrroline, and *β* signals were assigned similarly on the basis of the HMQC method (S-14, S-15, S-16). Figure 5b′ shows the ^{13}C NMR spectrum of *meso*-^{13}C-enriched complex. The strong signals at 293 and 262 ppm were assigned to the *meso* carbons. The other four signals with short relaxation times at 43, 31, −19, and −89 ppm were then assigned to the α carbons. Figure 2b shows the change in ^{13}C NMR chemical shifts when CD_3OD was added to the CD_2Cl_2 solution of $[Fe(TPC)(CN)_2]^-$. The titration experiment enables the correlation of the signals in CD_2Cl_2 solution to the corresponding signals in CD_3OD. As in the case of pyrrole-H signals, the spread of the pyrrole *β* signals decreased from 271 to 183 ppm as CD_2Cl_2 was replaced by CD_3OD.

$[Fe(TPC)(1\text{-}MeIm)_2]Cl$. Figure 6a shows the proton-coupled ^{13}C NMR spectra of $[Fe(TPC)(1\text{-}MeIm)_2]^+$ taken in CD_2Cl_2 solution at 298 K. Signal assignment of the carbons with directly bonded protons such as pyrroline-*β*, *o*, *m*, and *p* was carried out on the basis of the relative intensity and multiplicity of the signal in the proton coupled spectra together with the heteronuclear selective decoupling method. Thus, the broad doublets at 288, 113, and −23 ppm were assigned to the 8,17-C, 12,13-C, and 7,18-C, respectively, by the heteronuclear selective decoupling of the corresponding proton signals at −35, −10, and −1.0 ppm, respectively (S-17). As shown in Figure 6b, the *ipso* signals were discriminated from the α and *meso* signals by partially relaxed NMR spectra because the former signals were negative while the latter were positive when the spectrum was taken with the pulse interval 75 ms in the 180°−*τ*−90° pulse sequence. When the temperature was lowered to 273 K, the signal at −19 ppm split into two signals, indicating that they accidentally overlapped at 298 K. Thus, the five signals at 224, 171, 146, −19, and −91 ppm were assigned to either the *meso* or the α signals. We could unambiguously assign the signals at 146 and −19 ppm to the *meso* carbons by using *meso*-^{13}C-enriched $[Fe(TPC)(1\text{-}MeIm)_2]^+$ as shown in Figure 6c. Thus, the other 4 signals at 224, 171, −19, and −91 ppm were assigned to the α carbons.

$[Fe(TPC)(4\text{-}CNPy)_2]ClO_4$. Figure 7a shows the proton-coupled ^{13}C NMR spectra of $[Fe(TPC)(4\text{-}CNPy)_2]^+$ taken in CD_2Cl_2 solution at 253 K. The most downfield shifted signals, 476 and 486 ppm, were assigned to the *meso* signals since the *meso*-^{13}C-enriched $[Fe(TPC)(4\text{-}CNPy)_2]^+$ exhibits two signals at nearly the same positions as shown in Figure

Table 1. ^{1}H NMR Chemical Shifts of $[Fe(TPC)(L)_2]^{\pm}$ and $[Co(TPC)(L)_2]^{\pm}$ in CD_2Cl_2 at 298 K

complexes	pyrroline	7,18	8,17	12,13	*o*		*m*		*p*		ref
					$[Fe(TPC)L_2]^{\pm}$						
PMe_2Ph	64.6	0.7	−57.8	0.7	6.85	6.98	7.62	7.71	7.10	7.44	18
1-MeIm	39.1	−1.0	−35.0	−10.0	6.17	6.17	7.22	7.11	7.11	6.91	20
CN^-	25.8	3.3	−26.0	−1.9	6.38[d]	6.66[e]	7.94[d]	7.88[e]	6.95[d]	6.88[e]	this work
CN^- [a]	6.8	8.7	−10.8	2.3	5.80[d]	6.56[e]	9.62[d]	9.28[e]	6.63[d]	6.74[e]	this work
$P(OMe)_2Ph$	0.9	10.9	−11.5	5.6	3.7	4.4	11.55	11.2	5.8	5.65	21
4-CNPy	nd	14.4	−8.9	4.5	3.77[f]	4.60[g]	11.46[f]	10.87[g]	5.65[f]	5.60[g]	this work
4-CNPy[b]	−0.1	16.0	−6.6	4.4	2.76[f]	3.64[g]	12.54[f]	11.74[g]	5.17[f]	5.01[g]	this work
^{t}BuNC	−36.0	7.9[c]	5.1[c]	7.2	−0.39[f]	1.3[g]	14.7[f]	12.9[g]	3.07[f]	3.42[g]	19
					$[Co(TPC)L_2]^{\pm}$						
CN^-	4.00	8.08	8.36	8.28	7.81[d]	8.00[e]	7.56[d]	7.63[e]	7.58[d]	7.61[e]	this work

[a] In CD_3OD solution. [b] Data at 253 K. [c] The assignment of the signals at 7.9 and 5.1 ppm could be reversed. [d] Protons at 5,20-phenyl rings. [e] Protons at 10,15-phenyl rings. [f,g] Protons belong to the same phenyl group.

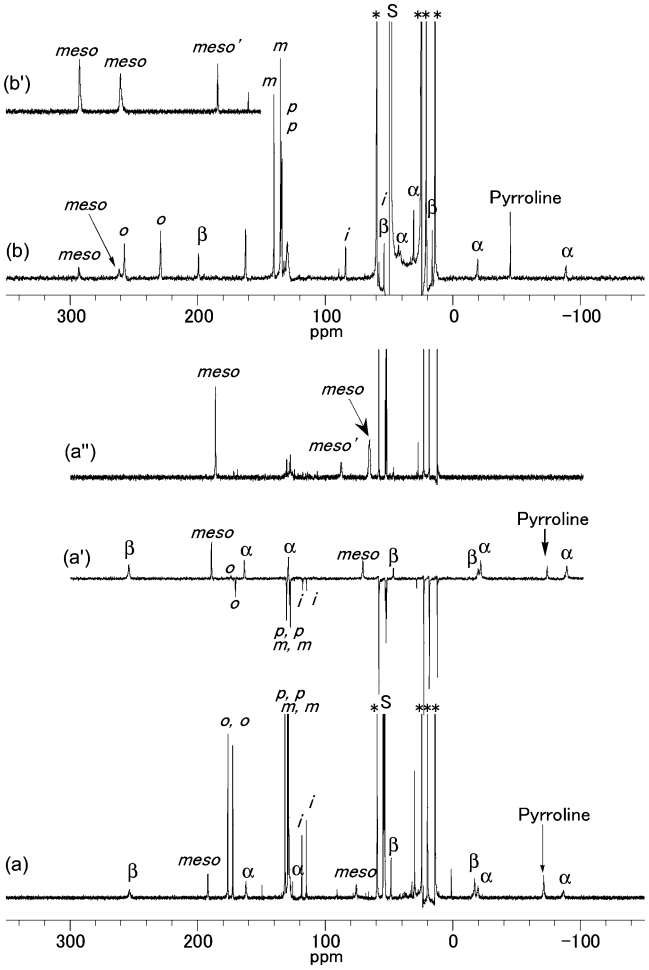

Figure 5. ^{13}C NMR spectra of $[Fe(TPC)(CN)_2]^-$ taken in (a) CD_2Cl_2 and (b) CD_3OD solutions at 298 K. Insets: (a′) partially relaxed spectrum; (a″) *meso*-^{13}C-enriched $[Fe(TPC)(CN)_2]^-$; (b′) *meso*-^{13}C-enriched $[Fe(TPC)(CN)_2]^+$. Signals signified by *meso*′ are ascribed to the *meso* signal of $[Fe(TPP)(CN)_2]^-$. The butyl signals of tetrabutylammonium cyanide are signified by asterisks.

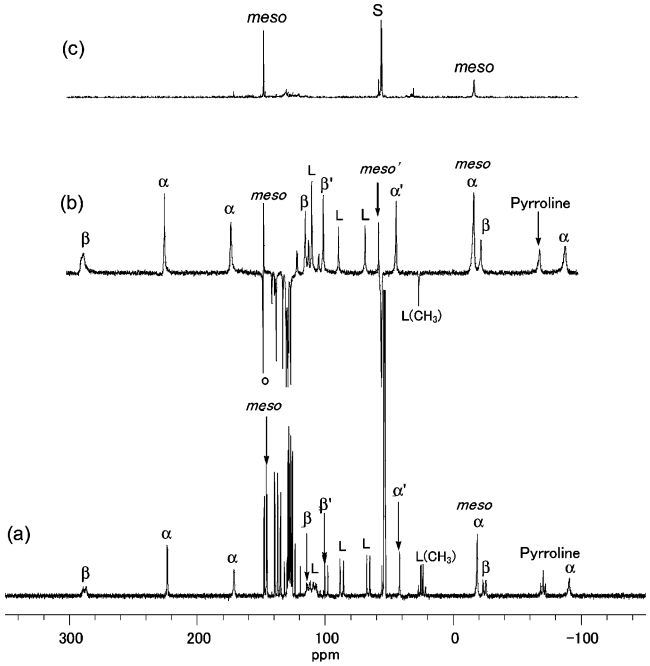

Figure 6. ^{13}C NMR spectrum of $[Fe(TPC)(1\text{-}MeIm)_2]^+$ taken in CD_2Cl_2 solution at 298 K: (a) proton-coupled ^{13}C NMR spectrum; (b) partially relaxed proton-decoupled ^{13}C NMR spectrum; (c) proton-decoupled ^{13}C NMR spectrum of *meso*-^{13}C-enriched complex. Signals signified by α′, β′, and *meso*′ are ascribed to $[Fe(TPP)(1\text{-}MeIm)_2]^+$.

7b. The α and *ipso* signals were discriminated by the spectral comparison of Figure 7c,d; Figure 7d shows the proton-coupled partially relaxed spectrum where the *ipso*-C exhibit negative signals due to the longer relaxation times as compared with the α-C.

$[Fe(TPC)(^t BuNC)_2]ClO_4$. Figure 8 shows the proton-coupled ^{13}C NMR spectrum of $[Fe(TPC)(^t BuNC)_2]^+$ taken in CD_2Cl_2 solution at 298 K. Signals were assigned similarly. Although we could not observe the *meso*-^{13}C signals by the conventional single pulse measurement even by using *meso*-^{13}C-enriched complex, two signals certainly appeared at 700 and 763 ppm as shown in the inset (a) when some strong signals were eliminated by the proton decoupled partially relaxed ^{13}C NMR spectrum. In the inset (b) is given the ^{13}C NMR spectrum of a narrow region between 0 and 40 ppm. The proton-coupled partially relaxed ^{13}C NMR spectrum shown in the inset (c) revealed that the methyl signals of the coordinated ^{t}BuNC exactly overlapped with the pyrroline signals. It should be noted that pyrroline-C signal appeared at +20 ppm while the corresponding signals of all the other complexes were observed at rather upfield positions, i.e. −25 to −71 ppm.

$[Co(TPC)(CN)_2]NBu_4$. Signal assignments of diamagnetic $[Co(TPC)(CN)_2]NBu_4$ were carried out by 1D and 2D NMR spectroscopy. Signal assignment of the carbons with directly bonded protons such as pyrroline-*β*, pyrrole-*β*, *o*, *m*, and *p*

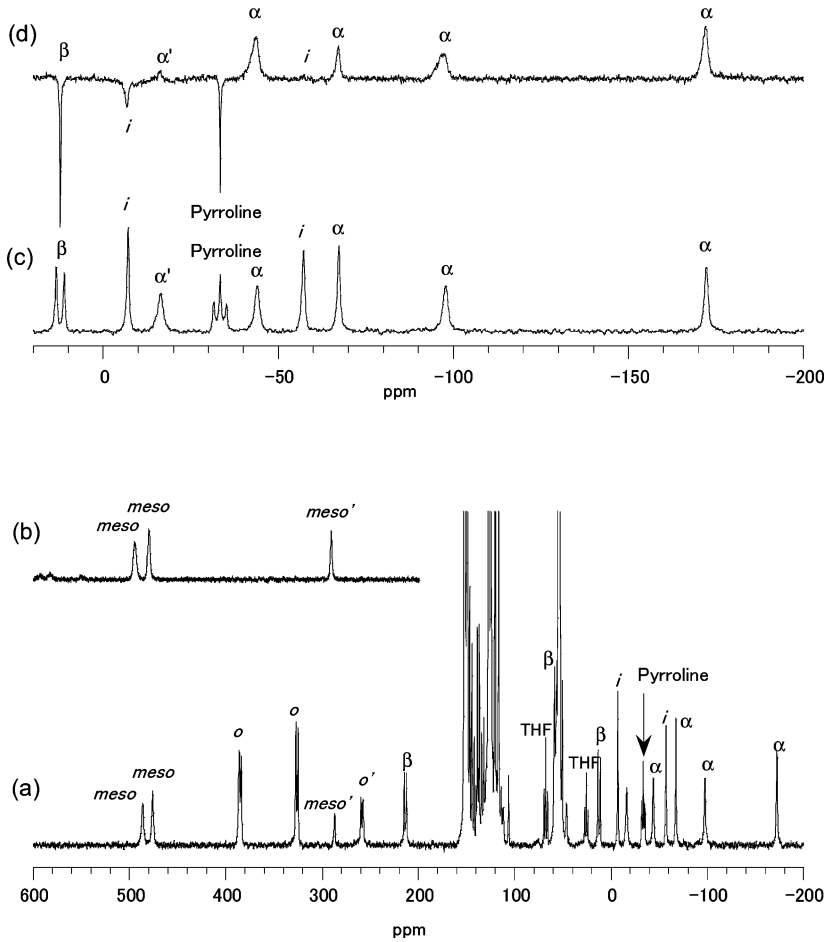

Figure 7. ^{13}C NMR spectra of $[Fe(TPC)(4\text{-}CNPy)_2]^+$ taken in CD_2Cl_2 solution at 253 K: (a) proton-coupled spectrum; (b) proton-decoupled spectrum of *meso*-^{13}C-enriched complex; (c) proton-coupled spectrum of −200 to 50 ppm region; (d) proton-decoupled partially relaxed spectrum of −200 to 50 ppm region.

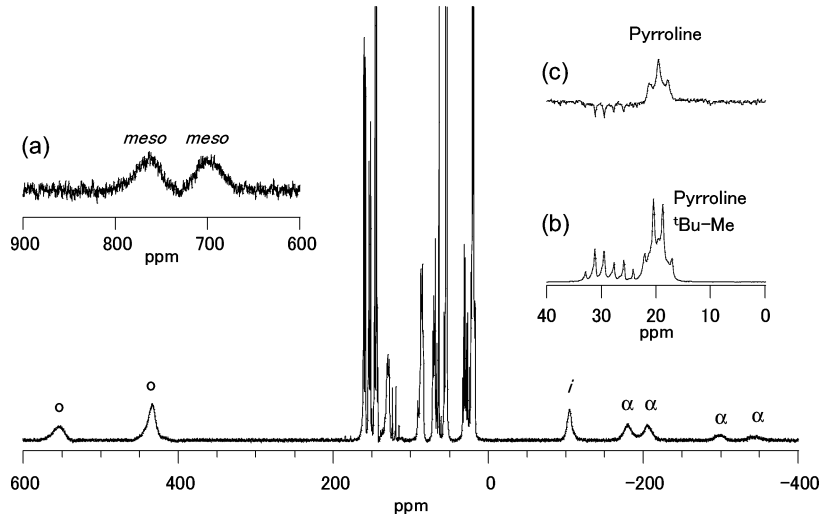

Figure 8. ^{13}C NMR spectra of $[Fe(TPC)(^tBuNC)_2]^+$ taken in CD_2Cl_2 solution at 298 K. Insets: (a) downfield region of the *meso*-^{13}C-enriched complex; (b) proton-coupled ^{13}C NMR spectrum between 0 and 40 ppm; (c) proton-decoupled partially relaxed ^{13}C NMR spectrum of the same region as (b).

were carried out on the basis of the $^1H\{^{13}C\}$ HMQC experiments. Thus, the signals at 128.2, 133.8, and 129.6 ppm were assigned to the 7,18-C, 8,17-C, and 12,13-C, respectively. Similarly, the signal at 34.8 ppm was assigned to the pyrroline-C. Signal assignment of the carbons without directly bonded protons such as *meso*, *ipso*, and α-C was done by the HMBC experiment. Thus, the signal at 109.9 ppm was assigned to the 5,20-C since it showed correlation peaks with the ^1H signals at 4.0 ppm (pyrroline-H) and 7.81 ppm (*ortho*-H) in the HMBC spectra (S-18). Similarly, the signal at 123.0 ppm was assigned to the 10,15-C since it showed a correlation peak with the ^1H signals at 8.00 ppm

Table 2. ^{13}C NMR Chemical Shifts of $[Fe(TPC)L_2]^{\pm}$ and $[Co(TPC)(CN)_2]^-$ in CD_2Cl_2 at 298 K[a]

(a) Chlorin Ring

complexes	pyrroline	meso		α				7,18	8,17	12,13
				$[Fe(TPC)L_2]^{\pm}$						
1-MeIm	−70	146 (56)	−19	224 (42)	171	−19	−91	−23 (99)	288	113 (99)
CN^-	−71	192 (89)	76	162 (41)	130	−20	−87	−17 (90)	254	48 (90)
CN^- [b]	−45	293 (184)	262	43 (27)	31	−19	−89	16 (89)	199	54 (89)
4-CNPy	−25	413 (243)	396	11 (46)	−19	−35	−129	20 (150)	222	77 (150)
4-CNPy[c]	−34	486 (289)	476	−44 (−17)	−67	−100	−172	12 (113)	213	57 (113)
^{t}BuNC	20	763 (767)	700	−179 (−294)	−204	−297	−342	85 (83)	70	86 (83)
				$[Co(TPC)L_2]^{\pm}$						
CN^-	35	110 (119)	123	155 (143)	147	139	142	128 (133)	134	130 (133)

(b) Phenyl Group

complexes	ipso	*o*		*m*		*p*	
			$[Fe(TPC)L_2]^{\pm}$				
1-MeIm	139	129 (137)	136	147 (131)	127	128 (125)	127	128 (126)
CN^-	118[d]	115[e] (127)	177[d]	173[e] (149)	129[d]	132[e] (125)	129[d]	130[e] (127)[f]
CN^- [b]	58[d]	84[e] (104)	258[d]	229[e] (195)	140[d]	135[e] (131)	134	134 (132)[f]
4-CNPy	−15	22 (74)	331	288 (225)	144	137 (132)	140	145 (137)
4-CNPy[c]	−57	−7 (46)	385	326 (259)	148	138 (133)	143	145 (139)
^{t}BuNC	−104	−104 (−123)	552	432 (458)	159	145 (146)	153	153 (155)[g]
			$[Co(TPC)L_2]^{\pm}$				
CN^-	142.7	131.8 (127)	132.8	133.9 (135)	127.9	127.5 (127)	127.2	127.2 (128)[f]

[a] Data in parentheses are the chemical shifts of the corresponding signals of $[Fe(TPP)L_2]^{\pm}$ and $[Co(TPP)(CN)_2]^-$. [b] In CD_3OD. [c] Data at 253 K. [d] Carbons at 5,20-phenyl rings. [e] Carbons at 10,15-phenyl ring. [f] Reference 42. [g] Reference 45.

(*ortho*-H). The signals at 142.7 and 141.8 ppm were assigned to the *ipso*-C since they showed the correlation peaks with the *meta*-H signals at 7.56 and 7.63 ppm, respectively. The signals at 154.5 and 141.7 ppm were assigned to the 1,4-C and 11,14-C, respectively, due to the presence of the correlation peaks at 4.00 (pyrroline-H) and 8.28 ppm (12,13-H), respectively. The other two signals, 147.1 and 138.8 ppm, were assigned to the 6,19-C and 9,16-C though the complete assignment is not successful at this point.

Table 2 shows the ^{13}C NMR chemical shifts of $[Fe(TPC)L_2]^{\pm}$ and $[Co(TPC)(CN)_2]^-$, where the axial ligands of $[Fe(TPC)L_2]^{\pm}$ are arranged in the same order as those in Table 1. The data in Table 2 clearly indicate that the pyrroline and *meso* carbon signals continuously move downfield as the axial ligand changes from 1-MeIm to ^{t}BuNC. The chemical shifts of the *meso*, α, *β*, and phenyl carbon signals of the corresponding porphyrin complexes, $[Fe(TPP)L_2]^{\pm}$ and $[Co(TPP)(CN)_2]^-$, taken under the same conditions are also listed in the parentheses of Table 2.[42]

Discussion

Electron Configurations of the Iron(III) Chlorinates. General Consideration. As shown in Scheme 1, there are two types of electronic ground states, $(d_{xy})^2(d_{xz}, d_{yz})^3$ and $(d_{xz}, d_{yz})^4(d_{xy})^1$, in low-spin iron(III) porphyrinates.[43] Extensive studies using NMR spectroscopy have revealed that not only the pyrrole-H but also the *meso*-C chemical shifts are powerful probes to elucidate the electronic ground state.[43−53] In the low-spin $[Fe(TPP)L_2]^{\pm}$ with the $(d_{xy})^2(d_{xz}, d_{yz})^3$ ground

Scheme 1. Two Types of Electronic Ground States

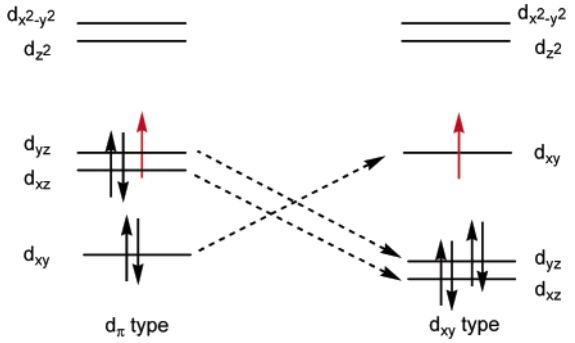

state, the complexes usually exhibit a nearly planar porphyrin ring. Both the pyrrole-H and *meso*-C signals appear at rather upfield positions due to the $d_\pi-3e_g$ interactions. This is because the $3e_g$ orbital has large coefficients at the *β* pyrrole and zero coefficient at the *meso* carbon atoms.[43] In the case

(42) Ikezaki, A.; Ikeue, T.; Nakamura, M. *Inorg. Chim.* Acta **2002**, *335*, 91−99.
(43) Walker, F. A. In *The Porphyrin Handbook*; Kadish, K. M., Smith, K. M., Guilard, R., Eds.; Academic Press: San Diego, CA, 2000; Vol. 5, Chapter 36, pp 81−183.
(44) Ikeue, T.; Ohgo, Y.; Saitoh, T.; Nakamura, M.; Fujii, H.; Yokoyama, M. *J. Am. Chem. Soc.* **2000**, *122*, 4068−4076.
(45) Ikeue, T.; Ohgo, Y.; Saitoh, T.; Yamaguchi, T.; Nakamura, M. *Inorg. Chem.* **2001**, *40*, 3423−3434.
(46) Ikeue, T,; Ohgo, Y.; Ongayi, O.; Vicente, M. G. H.; Nakamura, M. *Inorg. Chem.* **2003**, *42*, 5560−5571.
(47) Rivera, M.; Caignan, G. A. *Anal. Bioanal. Chem.* **2004**, *378*, 1464−1483.
(48) Hoshino, A.; Nakamura, M. *Chem. Commun.* **2005**, 915−917.
(49) Hoshino, A.; Ohgo, Y.; Nakamura, M. *Inorg. Chem.* **2005**, *44*, 7333−7344.
(50) Safo, M. K.; Walker F. A.; Raitsimring, A. M.; Walters, W. P.; Dolata, D. P.; Debrunner, P. G.; Scheidt, W. R. *J. Am. Chem. Soc.* **1994**, *116*, 7760−7770.
(51) Walker, F. A.; Nasri, H.; Turowska-Tyrk, I.; Mohanrao, K.; Watson, C. T.; Shokhirev, N. V.; Debrunner, P. G.; Scheidt, W. R. *J. Am. Chem. Soc.* **1996**, *118*, 12109−12118.
(52) Pilard, M.-A.; Guillemot, M.; Toupet, L.; Jordanov, J.; Simonneaux, G. *Inorg. Chem.* **1997**, *36*, 6307−6314.
(53) Simonneaux, G.; Schünemann, V.; Morice, C.; Carel, L.; Toupet, L.; Winkler, H.; Trautwein, A. X.; Walker, F. A. *J. Am. Chem. Soc.* **2000**, *122*, 4366−4377.

of the $(d_{xz}, d_{yz})^4(d_{xy})^1$ type complexes with D_{4h} symmetry, the d_{xy} orbital is orthogonal to any of the porphyrin frontier orbitals. Actually however, the low-spin complexes adopting the $(d_{xz}, d_{yz})^4(d_{xy})^1$ ground state almost always exhibit the ruffled structure.[50−53] Thus, the iron d_{xy} orbital can interact with the porphyrin a_{2u} orbital because both orbitals are signified as b_2 in the ruffled complexes with D_{2d} symmetry.[43,54,55] The interaction between these two orbitals should induce a large downfield shift of the *meso*-C signal since the a_{2u} orbital has a large coefficient at the *meso* carbon atoms. By contrast, the pyrrole-H signal appears close to the diamagnetic position despite the $a_{2u}-d_{xy}$ interaction, because the a_{2u} orbital has zero coefficient at the β pyrrole carbon atoms.[56] We have recently found the direct EPR evidence showing that low-spin $[Fe(TArP)(CN)_2]^-$ (Ar = 2,4,6-triethylphenyl) exists as an equilibrium mixture of the two isomers with different electronic ground states.[57] Because the energy gap between these two isomers is expected to be quite small, they are rapidly interconverting in solution as shown in eq 1.[57,58] Thus, the observed chemical shift of the nucleus i, signified by δ_i(obs), is expressed by eq 2, where $\delta_i(d_\pi)$ and $\delta_i(d_{xy})$ are the chemical shifts and $p(d_\pi)$ and $p(d_{xy})$ are the population of the isomers with the $(d_{xy})^2(d_{xz}, d_{yz})^3$ and $(d_{xz}, d_{yz})^4(d_{xy})^1$ ground state, respectively.[57] However, this aspect may be more complicated if we consider that excited states can be thermally populated, as it has been previously reported in some cases with low-spin iron(III) heme proteins and iron porphyrins.[32,59−62]

$$(d_{xy})^2(d_{xz}, d_{yz})^3 \overset{K}{\rightleftharpoons} (d_{xz}, d_{yz})^4(d_{xy})^1$$

$$\delta_i(\text{obs}) = p(d_\pi)\delta_i(d_\pi) + p(d_{xy})\delta_i(d_{xy}) \qquad (2)$$

The molecular orbitals of the chlorin ring are different from those of the porphyrin because of the reduction of one of the pyrrole rings. Recent theoretical work on the electronic structure of low-spin (octaethylchlorinato)iron(III) complexes with the $(d_{xy})^2(d_{xz}, d_{yz})^3$ ground state has shown that the A_{-1} and S_{-1} orbitals correspond to the $1a_{1u}(\pi)$ and $3a_{2u}(\pi)$ orbitals, respectively, in the D_{4h} porphyrin complexes.[32] Similarly, the A_{-2} and S_{-2} orbitals correspond to the $3e_g(y)$ and $3e_g(x)$ orbitals, respectively. These orbitals are shown in Chart 2. The important consequence from the calculation is that the d_{yz} orbital appears to interact almost equally with the two antisymmetric orbitals, A_{-2} and A_{-1}, because of the heavy mixing among metal d and chlorin π orbitals. In addition to these interactions, the d_{xy} orbital can interact with the S_{-1} orbital if the chlorin ring is ruffled as in the case of the porphyrin complexes.[32] The NMR chemical shifts listed in Tables 1 and 2 should be the results of orbital interactions mentioned above. Thus, we have determined the electronic structures of a series of complexes on the basis of the ^{1}H and ^{13}C NMR chemical shifts.

Chart 2. Hückel Frontier Orbitals of the Chlorin Ring for Low-Spin Fe(III) Complexes with $(d_{xy})^2(d_{xz}, d_{yz})^3$ Ground State Reported by Cai, Lichtenberger, and Walker[32] [a]

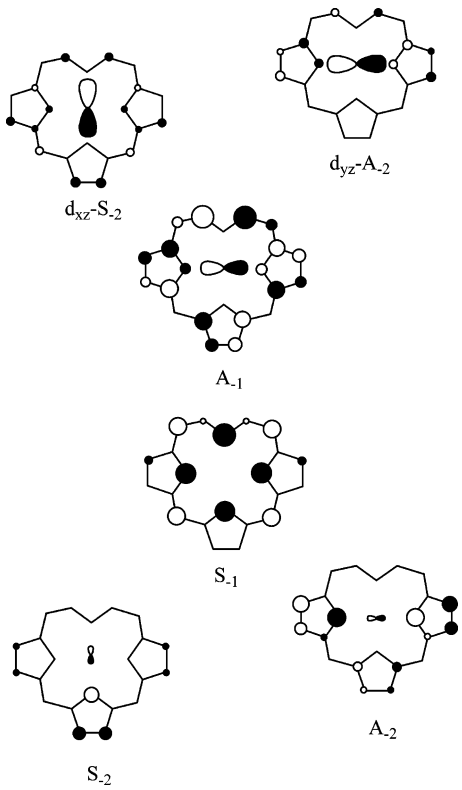

[a] The highest (singly) occupied orbital is $d_{yz}-A_{-2}$. A_{-1} and S_{-1} are analogues of the $1a_{1u}$ and $3a_{2u}$ orbitals of the porphyrin ring, respectively.

$[Fe(TPC)L_2]^+$ (L = PMe_2Ph, 1-MeIm). These complexes have been reported to adopt the $(d_{xy})^2(d_{xz}, d_{yz})^3$ ground state on the basis of the ^{1}H NMR and EPR spectroscopy as well as X-ray crystallography.[18,20] The ^{13}C NMR chemical shifts listed in Table 2 also support the $(d_{xy})^2(d_{xz}, d_{yz})^3$ ground state. The average chemical shift of the *meso* carbon signals of $[Fe(TPC)(1\text{-MeIm})_2]^+$ is 64 ppm, which is ca. 53 ppm more upfield than that of diamagnetic $[Co(TPC)(CN)_2]^-$. Among the six β-C, 8,17-C have the largest spin densities as is revealed from their largest downfield shift, 288 ppm, together with the largest upfield shift of the 8,17-H, −35.0 ppm, respectively. Thus, the major interactions that affect the ^{1}H and ^{13}C NMR chemical shifts in these complexes are the $d_{yz}-A_{-2}$ and to a minor extent the $d_{yz}-A_{-1}$ and $d_{xz}-S_{-2}$ interactions.

$[Fe(TPC)(CN)_2]^-$. The ^{1}H and ^{13}C NMR spectra of $[Fe(TPC)(CN)_2]^-$ shown in Figures 1 and 5 are quite similar to those of $[Fe(TPC)(1\text{-MeIm})_2]^+$ if they are taken in CD_2Cl_2 solution. The large upfield shift of the 8,17-H, −26 ppm, together with the large downfield shift of the pyrroline-

(54) Ghosh, A.; Gonzalez, E.; Vangberg, T. *J. Phys. Chem. B* **1999**, *103*, 1363−1367.
(55) Cheng, R.-J.; Chen, P.-Y.; Lovell, T.; Liu, T.; Noodleman, L.; Case, D. A. *J. Am. Chem. Soc.* **2003**, *125*, 6774−6783.
(56) Simonneaux, G.; Hindre, F.; Le Plouzennec, M. *Inorg. Chem.* **1989**, *28*, 823−825.
(57) Ikezaki, A.; Nakamura, M. *Inorg. Chem.* **2002**, *41*, 2761−2768.
(58) Rivera, M.; Caignan, G. A.; Astashkin, A. V.; Raitsimring, A. M.; Shokhireva, T.K.; Walker, F. A. *J. Am. Chem. Soc.* **2002**, *124*, 6077−6089.
(59) Kurland, R. J.; McGarvey, B. R. *J. Magn. Reson.* **1970**, *2*, 286−301.
(60) Shokhirev, N. V.; Walker, F. A. *J. Phys. Chem.* **1995**, *99*, 17795−17804.
(61) Banci, L.; Bertini, I.; Luchinat, C.; Pierattelli, R.; Shokhirev, N. V.; Walker, F. A. *J. Am. Chem. Soc.* **1998**, *120*, 8472−8479.
(62) Bertini, I.; Luchinat, C.; Giacomo, P. *Eur. J. Inorg. Chem.* **2000**, 2473−2480.

H, 25.8 ppm, clearly indicates that the complex also adopts the $(d_{xy})^2(d_{xz}, d_{yz})^3$ ground state. In other words, the isomer with the $(d_{xy})^2(d_{xz}, d_{yz})^3$ ground state predominantly exists in the equilibrium state. It should be noted that the population of the $(d_{xz}, d_{yz})^4(d_{xy})^1$ isomer in $[Fe(TPC)(CN)_2]^-$ is much larger than that in $[Fe(TPC)(1\text{-MeIm})_2]^+$ since the *meso*-C signals in the former complex appeared more downfield than those of the latter one.

Addition of CD_3OD to the CD_2Cl_2 solution of $[Fe(TPC)(CN)_2]^-$ greatly affects the chemical shifts of the pyrroline-H and *meso*-C signals as shown in Figure 2a,b; the pyrroline-H signal shifted upfield from 25.8 to 6.8 ppm while the *meso*-C signals shifted to the opposite direction from 192 and 76 ppm to 293 and 262 ppm. The large downfield shift of the *meso*-C signals suggests the increase in spin densities at the *meso* carbons caused by the interaction between S_{-1} and the half-filled d_{xy} orbital in a probably ruffled chlorin core. These results clearly indicate that the isomer with the $(d_{xz}, d_{yz})^4(d_{xy})^1$ ground-state predominates in CD_3OD solution. This is because the hydrogen bonding between CD_3OD and coordinating CN^- lowers the energy level of the $\pi^*(CN^-)$ orbital and stabilizes the d_{xz} and d_{yz} orbitals relative to the d_{xy} orbital. The same phenomenon was observed in the porphyrin complexes.[63−67] Figure 3a,b shows the Curie plots of the ^{1}H signals in $[Fe(TPC)(CN)_2]^-$ determined in CD_2Cl_2 and CD_3OD solutions, respectively. The large positive slope of the pyrroline-H signal in CD_2Cl_2 solution, $+2.7 \times 10^4$ ppm·K, changed to the negative one, -1.1×10^4 ppm·K, in CD_3OD solution, which is consistent with the large decrease in π spin densities at the pyrroline α-C. The fact that the 8,17-H and pyrroline-C signals still appear rather upfield positions, −10.8 and −45 ppm, respectively, suggests that a considerable amount of the $(d_{xy})^2(d_{xz}, d_{yz})^3$ isomer exists in the equilibrium state.

$[Fe(TPC)(4\text{-CNPy})_2]^+$. The ^{1}H NMR data in Table 1 suggest that the chemical shifts of $[Fe(TPC)(4\text{-CNPy})_2]^+$ are quite close to those of $[Fe(TPC)\{P(OMe)_2Ph\}_2]^+$ adopting the $(d_{xz}, d_{yz})^4(d_{xy})^1$ ground state.[21] The large downfield shifts of the *meso*-C signals, which reached 486 and 476 ppm, suggest the increase in positive spin at these carbon atoms caused by the interaction between S_{-1} and half-filled d_{xy} orbital. Correspondingly, the negative slope of the pyrroline-H Curie plots shown in Figure 3c increased to -1.3×10^4 ppm·K. The results indicate that the replacement of the axial cyanide ligand by 4-CNPy greatly stabilized the $(d_{xz}, d_{yz})^4(d_{xy})^1$ isomer. It should be noted, however, that the 8,17-H and pyrroline-C signals appeared rather upfield positions, −8.9 and −25 ppm, respectively. The results suggest that the population of the $(d_{xy})^2(d_{xz}, d_{yz})^3$ isomer is still not small.

$[Fe(TPC)(^tBuNC)_2]^+$. This complex is well characterized to adopt the $(d_{xz}, d_{yz})^4(d_{xy})^1$ ground state on the basis of the ^{1}H NMR, EPR, and X-ray crystallography.[19] The large upfield shift of the pyrroline-H signal, −36.0 ppm, suggests that the pyrroline α-C has a sizable amount of negative spin. Corresponding to a large upfield shift of the pyrroline-H signal, this complex exhibited the pyrroline-C signal at fairly downfield position, 20 ppm. The result again indicates that the π spin density at the pyrroline α-C has changed from a large positive to a negative value as the axial ligand changes from 1-MeIm to ^{t}BuNC. We expected, however, that the pyrroline-C signal of $[Fe(TPC)(^tBuNC)_2]^+$ should appear much more downfield than the corresponding signal of diamagnetic $[Co(TPC)(CN)_2]^-$, 34.8 ppm, because of the presence of negative spin at the neighboring α-C's. The smaller downfield shift could be explained in terms of the cancellation of the contact contribution to the pyrroline-C signal due to the negative spin at the two adjacent α-C's. That is, the downfield shift of the pyrroline-C caused by the negative spin at the directly bonded α-C is canceled by the upfield shift caused by the negative spin at the other α carbon atom.

As shown in the data in Tables 1 and 2, the chemical shifts of all the pyrrole-H and β-C in $[Fe(TPC)(^tBuNC)_2]^+$ are much closer to their diamagnetic positions than those of any other complexes examined in this study. The results suggest that the spin densities at the β-C are quite small in $[Fe(TPC)(^tBuNC)_2]^+$. The most characteristic feature in the ^{13}C NMR spectrum is the large downfield shifts of the *meso*-C signals, 763 and 700 ppm, which are ascribed to the large amount of spin densities at these carbons caused by the strong interaction between the S_{-1} and half-filled d_{xy} orbital. In contrast, all the neighboring carbons that are directly attached to the *meso*-C exhibited the signals at significantly upfield positions; the α- and *ipso*-C signals appeared at −179 to −342 ppm and at −104 ppm, respectively. This is because the large π spin densities at the *meso* carbon atoms polarize the adjacent $C_{meso}-C_\alpha$ and $C_{meso}-C_{ipso}$ bonds.[68,69]

Curie Plots of the Carbon Signals. Figure 9A shows the Curie plots of the *meso*-, α-, β-, and pyrroline-C signals of a series of $[Fe(TPC)L_2]^\pm$, where L's are (a) 1-MeIm, (b) CN^- (in CD_2Cl_2), (c) CN^- (in CD_3OD), and (d) 4-CNPy. Curie plots of the ^{t}BuNC complexes were not available because the signals were too broad to detect at lower temperatures. In Figure 9A, the Curie plots of the *meso* signals are expressed by the red filled circle. They exhibited a good linearity though the intercepts at $1/T = 0$ deviated from the corresponding diamagnetic values. The average slopes and the intercepts for these complexes are as follows: (a) -3.3×10^4 ppm·K, 175 ppm; (b) -6.0×10^4 ppm·K, 338 ppm; (c) 10×10^4 ppm·K, −62.5 ppm; (d) 13×10^4 ppm·K, −16.1 ppm. The slopes of the Curie plots clearly

(63) Nakamura, M.; Ikeue, T.; Fujii, H.; Yoshimura, T. *J. Am. Chem. Soc*. **1997**, *119*, 6284−6291.
(64) Nakamura, M.; Ikeue, T.; Fujii, H.; Yoshimura, T.; Tajima, K. *Inorg. Chem*. **1998**, *37*, 2405−2414.
(65) Wołowiec, S.; Latos-Grażyński, L.; Mazzanti, M.; Marchon, J.-C. *Inorg. Chem.* **1997**, *36*, 5761−5771.
(66) Wołowiec, S.; Latos-Grżyński, L.; Toronto, D.; Marchon, J.-C. *Inorg. Chem.* **1998**, *37*, 724−732.
(67) La Mar, G. N.; Gaudia, J. D.; Frye, J. S. *Biochim. Biophys. Acta* **1977**, *498*, 422−435.
(68) Goff, H. M. Nuclear Magnetic Resonance of Iron Porphyrins. In *Iron Porphyrins, I*; Lever, A. B. P., Gray, H. B., Eds.; Physical Bioinorganic Chemistry Series 1; Addison-Wesley: Reading, MA, 1983; pp 237−281.
(69) Bertini, I.; Luchinat, C. In *NMR of Paramagnetic Substances*; Lever, A. B. P., Ed.; Coordination Chemistry Reviews 150; Elsevier: Amsterdam, 1996; pp 29−75.

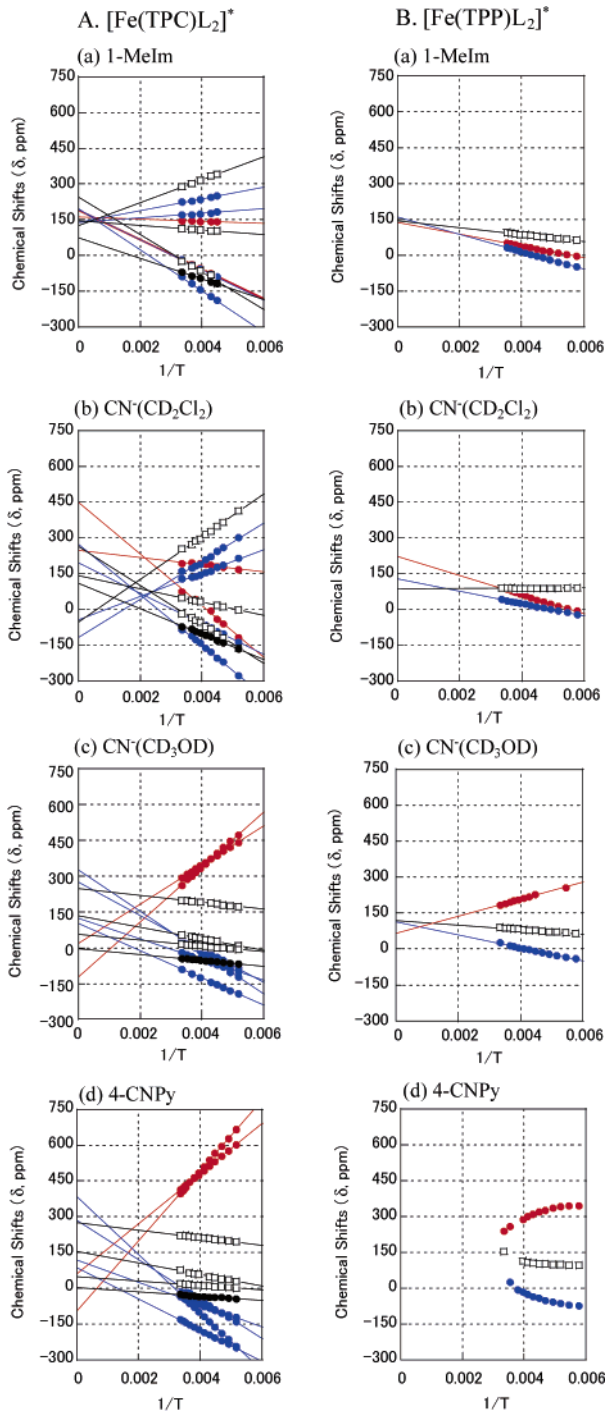

Figure 9. Curie plots of the carbon signals in a series of (A) $[Fe(TPC)L_2]^{\pm}$ and (B) $[Fe(TPP)L_2]^{\pm}$, where red-, blue-, and black-filled circles represent the *meso*, α, and pyrroline signals, respectively, and the open square indicates the *β* signals.

indicate that the 1-MeIm and CN^- (in CD_2Cl_2) complexes exist mainly as the $(d_{xy})^2(d_{xz}, d_{yz})^3$ isomer while the CN^- (in CD_3OD) and 4-CNPy complexes exist mainly as the $(d_{xz}, d_{yz})^4(d_{xy})^1$ isomer. One of the reasons for the deviation from the diamagnetic positions in these complexes should be ascribed to the temperature dependence of the equilibrium constant given in eq 1. Thus, the positive deviation of the *meso* signals in the 1-MeIm and CN^- (in CD_2Cl_2) complexes should be ascribed to the increase in population of the $(d_{xz}, d_{yz})^4(d_{xy})^1$ isomer at higher temperature. Similarly, the negative deviation in the CN^- (in CD_3OD) and 4-CNPy complexes should be ascribed to the increase in population of the $(d_{xy})^2(d_{xz}, d_{yz})^3$ isomer at higher temperature. Another notable feature in Figure 9A is the difference in spread of the pyrrole *β* chemical shifts given by black open circles. While the maximum differences in the chemical shifts of the *β* signals were 461 and 458 ppm at 223 K for the 1-MeIm and CN^- (in CD_2Cl_2) complexes, respectively, they were 183 and 197 ppm at the same temperature for the CN^- (CD_3OD) and 4-CNPy complexes, respectively. The result suggests that the spin densities at the peripheral *β*-C are quite different in the former complexes adopting the $(d_{xy})^2(d_{xz}, d_{yz})^3$ ground state while they are not much different in the latter complexes with the $(d_{xz}, d_{yz})^4(d_{xy})^1$ ground state. Similarly, while the differences in the chemical shifts of the *meso* signals were 230 and 221 ppm at 223 K for the 1-MeIm and CN^- (in CD_2Cl_2) complexes, they were only 8 and 34 ppm for the CN^- (CD_3OD) and 4-CNPy complexes, respectively. The differences in chemical shifts among the nonequivalent *β*-C and *meso*-C signals clearly indicate that the A_{-1} and A_{-2} orbitals in Chart 2 interact with the singly occupied d_{yz} orbital in $[Fe(TPC)(1\text{-}MeIm_2)]^+$ and $[Fe(TPC)(CN)_2]^-$ (in CD_2Cl_2) while the S_{-1} orbital mainly involves in the interaction with the singly occupied d_{xy} orbital in $[Fe(TPC)(CN)_2]^-$ (in CD_3OD) and $[Fe(TPC)(4\text{-}CNPy)_2]^+$.

Comparison with the Analogous Complexes. First, we have compared the electronic structures of the TPC complexes with those of the TPP complexes. Table 2 shows the ^{13}C NMR chemical shifts of a series of $[Fe(TPC)L_2]^{\pm}$ and $[Fe(TPP)L_2]^{\pm}$. As mentioned, the presence of the unpaired electron in the d_{xy} orbital induces the large downfield shift of the *meso* signal together with the large increase in the Curie slopes. Thus, the electronic structures of $[Fe(TPC)L_2]^{\pm}$ were compared with those of $[Fe(TPP)L_2]^{\pm}$ in terms of the *meso* carbon chemical shifts and the Curie slopes. Figure 9B shows the Curie plots of the *meso*, α, and *β* carbon signals of a series of $[Fe(TPP)L_2]^{\pm}$, where L's are (a) 1-MeIm, (b) CN^- (in CD_2Cl_2), (c) CN^- (in CD_3OD), and (d) 4-CNPy. As in the case of the chlorin complexes, the *meso* signal of the 1-MeIm and the CN^- (in CD_2Cl_2) complexes showed a positive deviation, while that of the CN^- (in CD_3OD) complex showed a negative deviation. In the case of the 4-CNPy complex, the Curie plots showed a considerable curvature. We observed a similar temperature dependence of the *meso* signals in some highly saddled complexes with weak nitrogen bases such as $[Fe(OETPP)(Py)_2]^+$ and $[Fe(OMTPP)(4\text{-}CNPy)_2]^+$.[46,70] The phenomenon was ascribed to the spin transition between $S = 3/2$ and $S = 1/2$. Thus, the curvature of the Curie plots in $[Fe(TPP)(4\text{-}CNPy)_2]^+$ could be explained in terms of the equilibrium among $(d_{xz}, d_{yz})^4(d_{xy})^1$, $(d_{xy})^2(d_{xz}, d_{yz})^3$, and $S = 3/2$. The slopes and intercepts of $[Fe(TPP)L_2]^{\pm}$ are (a) -2.5×10^4 ppm·K, 138 ppm, (b) -4.0×10^4 ppm·K, 222 ppm, (c) 3.8×10^4 ppm·K, 57 ppm, and (d) 3.2×10^4 ppm·K, 170 ppm; the curved plots in (d) was treated as a linear line. Thus, the

(70) Ikeue, T.; Ohgo, Y.; Yamaguchi, T.; Takahashi, M.; Takeda, M.; Nakamura, M. *Angew. Chem., Int. Ed.* **2001**, *40*, 2617−2620.

slopes of the CN^- (in CD_3OD) and 4-CNPy complexes in TPC are 3−4 times larger than those of the corresponding TPP complexes. In addition to the Curie slopes, the *meso* carbon signals of $[Fe(TPC)(CN)_2]^-$ (in CD_3OD) and $[Fe(TPC)(4\text{-}CNPy)_2]^+$ always appeared more downfield than those of the corresponding TPP complexes. These results clearly indicate that the TPC core stabilizes the $(d_{xz}, d_{yz})^4(d_{xy})^1$ isomer more effectively than the TPP core. The result should be ascribed to the flexible nature of the chlorin ring as compared with the porphyrin ring.[71] In contrast to the case of the CN^- and 4-CNPy complexes, the spin densities at the *meso* carbons in $[Fe(TPC)(^tBuNC)_2]^+$ and $[Fe(TPP)(^tBuNC)_2]^+$ are supposed to be quite close because the *meso* signals of the TPC and TPP complexes appeared at 732 (on average) and 767 ppm, respectively. Thus, both $[Fe(TPP)(^tBuNC)_2]^+$ and $[Fe(TPC)(^tBuNC)_2]^+$ exclusively exist as the $(d_{xz}, d_{yz})^4(d_{xy})^1$ isomer.

Secondary, we have compared the electronic structures of the TPC complexes with those of the OEC complexes reported by Cai and co-workers.[32] The largest difference was observed in the spin densities of the pyrroline α carbon atoms between $[Fe(TPC)(^tBuNC)_2]^+$ and $[Fe(OEC)(^tBuNC)_2]^+$. While $[Fe(TPC)(^tBuNC)_2]^+$ showed the pyrroline-H signal at −36 ppm at 298 K,[19] $[Fe(OEC)(^tBuNC)_2]^+$ exhibited the corresponding signal at 128 ppm at 213 K; this signal appears at ca. 140 ppm at 298 K as is revealed from Figure 11 of ref 32. The result indicates that the pyrroline α carbons have considerable amount of positive spin in $[Fe(OEC)(^tBuNC)_2]^+$ while they have negative spin in $[Fe(TPC)(^tBuNC)_2]^+$. Although the pyrroline α spin densities are quite different, these complexes commonly have large positive spin at the *meso* carbons as is revealed from the downfield shift of the *meso*-C and the upfield shift of the *meso*-H signals. Cai and co-workers explained the unusual spin distribution in $[Fe(OEC)(^tBuNC)_2]^+$ in terms of the rapidly interconverting equilibrium mixture between planar and ruffled structures; the unpaired electron occupies predominantly the d_{yz} orbital in the planar complex and the d_{xy} orbital in the ruffled one.[32] This is in sharp contrast to the case of $[Fe(TPC)(^tBuNC)_2]^+$, which exists exclusively as the probably ruffled $(d_{xz}, d_{yz})^4(d_{xy})^1$ isomer. The difference should again be ascribed to the flexible nature of the TPC ring as compared with the OEC ring. Immediately after we submitted this paper, a paper written by Cai and co-workers appeared on the Web, which discussed the ^1H NMR and EPR spectra of $[Fe(TPC)L_2]^+$ where L = imidazole-d_4, 2-methylimidazole, 4-(*N*,*N*-dimethylamino)pyridine, pyridine, and 4-CNPy.[72]

Conclusions

^{13}C NMR spectra of a series of low-spin chlorin complexes $[Fe(TPC)L_2]^{\pm}$ (L = 1-MeIm, CN^-, 4-CNPy, and ^{t}BuNC) have been examined to reveal the electronic structure. The signal assignments have been done on the basis of the relative signal intensity, signal multiplicity, homo- and heteronuclear selective decoupling, partially relaxed ^{13}C NMR spectra, and NOE difference spectra together with the 2D COSY and HMQC measurements. The *meso*-^{13}C-enriched complexes have been used successfully for the unambiguous assignments of the *meso* carbon signals. As in the case of the corresponding porphyrin complexes $[Fe(TPP)L_2]^{\pm}$, the contribution of the $(d_{xz}, d_{yz})^4(d_{xy})^1$ ground state has increased as the axial ligand changes from 1-MeIm, to CN^- (in CD_2Cl_2 solution), CN^- (in CD_3OD solution), and 4-CNPy, and then to ^{t}BuNC. In the case of the CN^- complex, the population of the $(d_{xz}, d_{yz})^4(d_{xy})^1$ isomer has increased to a great extent when the solvent is changed from CD_2Cl_2 to CD_3OD, which is ascribed to the hydrogen bonding between the coordinated cyanide ligand and methanol. While the 1-MeIm and CN^- (in CD_2Cl_2 solution) complexes exist almost exclusively as the $(d_{xy})^2(d_{xz}, d_{yz})^3$ isomer, the CN^- (in CD_3OD solution) and the 4-CNPy complexes exist as the mixture of the isomers with the $(d_{xy})^2(d_{xz}, d_{yz})^3$ and $(d_{xz}, d_{yz})^4(d_{xy})^1$ ground state. In the case of $[Fe(TPC)(^tBuNC)_2]^+$, the *meso*-C signals appeare extremely downfield, 763 and 700 ppm, while all the pyrrole-H signals are observed quite close to their diamagnetic positions. Thus, the ^{t}BuNC complex is considered to exist exclusively as the $(d_{xz}, d_{yz})^4(d_{xy})^1$ isomer. Because of the large positive spin at the *meso* carbon atoms, the pyrroline α carbons of this complex have negative spin, which induces the large upfield shift of the pyrroline-H, −36.0 ppm, together with the downfield shift of the pyrroline-C signal. Comparison of the spectral data between $[Fe(TPC)L_2]^+$ and $[Fe(TPP)L_2]^+$ has revealed that the population of the $(d_{xz}, d_{yz})^4(d_{xy})^1$ isomer is much larger in the TPC than in the TPP complex if the axial ligand is CN^-(in CD_3OD solution) or 4-CNPy, which is partly ascribed to the flexible nature of the chlorin core as compared with the porphyrin core. If the axial ligand is ^{t}BuNC, both $[Fe(TPC)(^tBuNC)_2]^+$ and $[Fe(TPP)(^tBuNC)_2]^+$ exist exclusively as the $(d_{xz}, d_{yz})^4(d_{xy})^1$ isomer. Recently, Cai and co-workers have suggested that $[Fe(OEC)(^tBuNC)_2]^+$ exists as a mixture of the planar and ruffled conformations with the unpaired electron predominantly in the d_{yz} and d_{xy} orbitals, respectively.[32] Thus, the present study reveals that the TPC complexes stabilizes the $(d_{xz}, d_{yz})^4(d_{xy})^1$ ground state more effectively than the TPP, OEC, and OEP complexes carrying the same axial ligands.

Acknowledgment. This work was supported by the Project Research Grant (No.17-12 to A.I.) of Toho University School of Medicine and by the Grant in Aid (No. 16550061 to M.N.) for Scientific Research from the Ministry of Education, Culture, Sports, Science, and Technology of Japan.

Supporting Information Available: Listing of homonuclear and heteronuclear selective decoupling, NOE difference spectra, and 2D COSY, HMQC, and HMBC spectra of a series of low-spin $[Fe(TPC)L_2]^{\pm}$ and diamagnetic $[Co(TPC)(CN)_2]^-$. This material is available free of charge via the Internet at http://pubs.acs.org.

IC060508O

(71) Stolzenberg, A. M.; Haymond, G. S. *Inorg. Chem.* **2002**, *41*, 300−308.
(72) Cai, S.; Shokhireva, T. K.; Lichtenberger, D. L.; Walker, F. A. *Inorg. Chem.* **2006**, *45*, 3519−3531.